Channel Modeling for UCA and URA Massive MIMO Systems

Xudong Cheng, Yejun He* and Jian Qiao
Guangdong Engineering Research Center of Base Station Antennas and Propagation
Shenzhen Key Laboratory of Antennas and Propagation
College of Electronics and Information Engineering, Shenzhen University, 518060, China
Email: cxd199181@126.com, heyejun@126.com*, 446941582@qq.com

***Abstract*—In this paper, we change the geometric structure of antenna array and extend our previous channel model of massive MIMO system with uniform linear array (ULA) to that of massive MIMO systems with uniform circular array (UCA) and uniform rectangular array (URA). Three massive MIMO systems with UCA, URA and ULA antenna array structures are named as UCA, URA and ULA Massive MIMO Systems, respectively, whose performance are analyzed and compared. The ULA massive MIMO system can make full use of space degree of freedom due to the large antenna array to achieve the best performance, however it is very difficult to be installed and placed on Base Station (BS) due to the large antennas array. The UCA massive MIMO system outperforms the URA massive MIMO system in many communication scenarios. The URA massive MIMO system is also sensitive to the elevation angle spread (EAS) by developing the degree of freedom in the vertical direction, and the spherical wave (SW) effect is very weak for URA antenna array because of the compact antenna structure. Finally, we give some guidelines for choosing the appropriate antenna array structures according to the communication scenarios and requirements.**

***Index Terms*—Massive MIMO, 5G, channel model, UCA, URA.**

I. Introduction

In recent years, the massive MIMO (Multi-Input Multi-Output) technology has attracted wide attention from academia and industry because it can greatly improve the spectral efficiency without increasing the spectrum resources and the total transmitting power, which is regarded as the core candidate technology of 5G (5th Generation) and it can be also used in the next generation WiFi [1], B5G (beyond 5G) or even 6G (6th Generation) [2]. Wireless mobile channel study is the basis of performance analysis in wireless mobile communication system, which is also the most basic and important part for massive MIMO system research. To understand and master the channel characteristics of the massive MIMO system and to establish the channel model for the massive MIMO system are essential for choosing appropriate system architecture, a reasonable communication scheme and improving system performance.

Massive MIMO system has a large number of antennas at base station (BS) that is serving several single-antenna users simultaneously, which has quite different channel characteristics from traditional MIMO systems. So far, there are a lot of works focused on massive MIMO system channel modeling. A theoretical non-stationary 3D wideband twin-cluster channel model for massive MIMO system was proposed in [3]. This model mainly focused on the non-stationary and spherical wave (SW) effect with uniform linear array (ULA) antennas at both transmitter and receiver. The authors used survival probability to describe the appearance and disappearance of clusters, the further apart the two antennas are, the less probability they will receive signals from the same cluster, which is called birth-death process. In [4], a non-stationary wideband multi-confocal ellipse 2D channel model was proposed, where the nth cluster is on the nth ellipse. Xie *et al.* [5] proposed a 3D two-cylinder regular-shaped model for non-isotropic scattering massive MIMO system channel. In this model, all the scatters are distributed on the surface of a cylinder and each antenna has its own 3D visible area by setting a virtual sphere. When the distance between a cluster and an antenna is less than the radius of the sphere, the cluster can be seen, hence different antennas will receive signals from different clusters to characterize the array non-stationarity. Wu *et al.* [6] proposed a novel Kronecker-based stochastic model for massive MIMO system channel and also used birth-death process to model the evolution of scatterers. A novel 2D non-stationary wideband model for massive MIMO system was proposed in [7]. In this model, the near-field effect was modeled by a second-order approximation to SW, which was called parabolic wavefront. Subsequently, the authors extended the model in [7] to 3D channel model in [8] and compared it with the channel measurements. Liu *et al.* [9] focused on the SW effect study and investigated the channel capacity of ULA massive MIMO system in LoS scenario, and both point-to-point (P2P) and multi-user (MU) massive MIMO system were considered. Chen *et al.* [10] proposed a novel twin-multi-ring channel model for massive MIMO system, where a new cluster generation algorithm based on birth-death process is proposed to describe the appearance and disappearance of clusters.

The main contributions of this paper are summarized as follows.

1) Since the existing massive MIMO system channel models only care about linear array and the structures of the antennas array directly affecting the system performance [11], we change the geometric structure of the antennas

978-1-7281-4905-9/20/$31.00 ©2020 IEEE

and extend our previous ULA massive MIMO system channel model in [12] to other two popular massive MIMO systems antennas array structures, i.e., uniform circular array (UCA) and uniform rectangular array (URA) to make full use of space degree of freedom and establish 3D geometrical channel models for them. Reference [12] only considered the linear array, while this paper gives a broader comparison.

2) The proposed channel models comprise the parameters of communication environment and antennas such as scattering status, near-field effect, antennas array structures etc, which can be adjusted according to the communication environment and are easily implemented. The proposed models are compared with measurements for validation.
3) The performances of three kinds of antenna arrays for massive MIMO systems are analyzed and compared, and some guidelines for choosing the appropriate antennas array structures are presented according to the communication scenarios and requirements.

The rest of this paper is organized as follows. 3D geometrical channel modeling for UCA massive MIMO system using SW is presented in Section II. In Section III, the URA massive MIMO system channel is modeled. Section IV presents the simulation results and analysis. Finally, we conclude the paper in Section V.

II. 3D Geometrical Channel Modeling for UCA massive MIMO system

In our paper, we assume a massive MIMO system has a BS equipped with M antennas is serving K ($K < M$) single-antenna users (users equipped with multiple antennas will be discussed in the future) at the same time in the same cell. According to [13], the channel matrix can be defined as

$$\mathbf{H} = [\mathbf{h}_1, \mathbf{h}_2 ... \mathbf{h}_k ... \mathbf{h}_K] \in \mathbb{C}^{M \times K} \tag{1}$$

where $\mathbf{h}_k = [h_{1,k}, h_{2,k} ... h_{m,k} ... h_{M,k}]^T$ is the channel vector of user k, and $h_{m,k}$ is the complex channel gain between BS antenna m and user k. Many studies and researches show that the favorable propagation characteristic (i.e., channel orthogonality between different users) is the most important property in massive MIMO system [11]

$$\frac{1}{M}\mathbf{h}_p^H \mathbf{h}_q \xrightarrow[M\to\infty]{a.s.} \begin{cases} 0, & p \neq q \\ 1, & p = q \end{cases} \tag{2}$$

where H denotes the Hermitian transform and $\xrightarrow{a.s.}$ is almost sure convergence. The favorable propagation can reduce the interference between users and simplify the precoding and signal detection algorithm of massive MIMO system, and in [14] the channel orthogonality between two users can be computed as

$$\delta_{p,q} = \frac{|(\mathbf{h}_p)^H \mathbf{h}_q|}{||\mathbf{h}_p|| \cdot ||\mathbf{h}_q||} \tag{3}$$

where $||\cdot||$ denotes the Euclidean norm. According to the theoretical study in [15], the channel capacity of massive MIMO system is given by [15]

$$C = \max_{\mathbf{P}} log_2[det(\mathbf{I} + \frac{\rho K}{M}\mathbf{HPH}^H)] \tag{4}$$

where ρ is the signal-to-noise ratio (SNR), and $\mathbf{I}$ is a identity matrix. $\mathbf{P}$ is a diagonal matrix with elements $(p_1 ... p_k ... p_K)$ satisfying $\sum_{k=1}^{K} p_k = 1$ for power allocation.

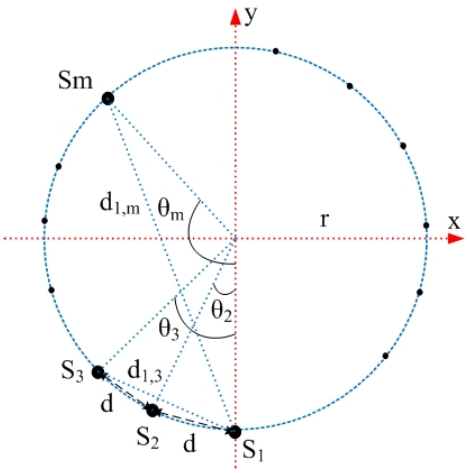

Fig. 1. Antenna array structure of UCA massive MIMO system.

UCA antennas are widely used in massive MIMO system because they are easily implemented and placed, where all the antennas are uniformly-spaced on a circular edge in UCA massive MIMO system as shown in Fig. 1. Fig. 1 is the top view and the antenna A_m is placed in the position S_m. All the antennas are placed in the horizontal plane with adjacent antenna spacing d. From Fig. 1 we can get $\theta = \frac{2\pi}{M}, \theta_2 = \theta, \theta_3 = 2\theta, ..., \theta_m = (m-1)\theta$, and the circle radius r is

$$r = \frac{d}{2sin(\theta/2)} \tag{5}$$

The distances between antenna A_1 and another antenna A_m are

$$d_{1,m} = \frac{dsin(\theta_m/2)}{sin(\theta/2)} \tag{6}$$

To make analysis tractable, we first analyze the relationship between antennas A_1 and A_m as shown in Fig. 2. We regard x-S_1-y plane as the horizontal plane and the antenna spacing is $d_{1,m}$. The signals come from different direction with azimuth angles of arrival (AAoA) $\alpha^X (X \in \{1, 2...M\}$ and elevation angles of arrival (EAoA) $\beta^X (X \in \{1, 2...M\}$. S is the last scattering point, $S^{'}$ is the projection of S on the horizontal plane x-S_1-y. The distance between the $S^{'}$ and the x axis is d_y, the distance between the $S^{'}$ and the y axis is d_x, and the height of S is h. From Fig. 2 we can see that the signals at the antennas are sphere, and the exact distances between the signal scattering point S and two antennas are

$$\begin{aligned} SS_1 &= \sqrt{(d_x^2 + d_y^2 + h^2)} \\ SS_m &= \sqrt{(S_1S_m' + d_x)^2 + (d_y - S_mS_m')^2 + h^2} \end{aligned} \tag{8}$$

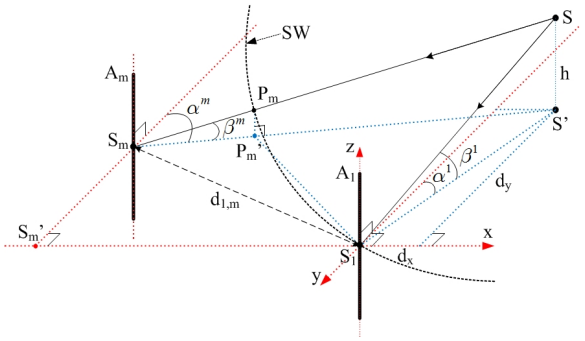

Fig. 2. 3D UCA massive MIMO system communication scenario using SW.

where $S_m^{'}S_1$, $S_mS_m^{'}$ are the functions of the number of antennas and antenna spacing. Then for different antennas we have

$$S_2^{'}S_1 = rsin\theta_2, S_2S_2^{'} = r - rcos\theta_2$$
$$...$$
$$S_m^{'}S_1 = rsin\theta_m, S_mS_m^{'} = r - rcos\theta_m \quad (9)$$

Regarding antenna A_1 as a reference antenna, one path of multipath channels (may be the nth path channel of the N multipath channels and we omit nth notation for sample expressions) at antennas A_1 and A_m of UCA massive MIMO system can be expressed as

$$h_1^{UCA} = Ae^{j(\phi+2\pi\sqrt{d_x^2+d_y^2+h^2}/\lambda)} \quad (10)$$

$$h_m^{UCA} = Ae^{j(\phi+2\pi\sqrt{(rsin\theta_m+d_x)^2+[d_y-(r-rcos\theta_m)]^2+h^2}/\lambda)} \quad (11)$$

where A is the receiving amplitude, ϕ is the receiving random phase with uniform distribution on the interval $[-\pi, \pi)$ [16]. According to the geometrical relationship in Fig. 2 we can get

$$d_x = tan(\alpha^m) * [d_y - (r - rcos\theta_m)] - rsin\theta_m$$
$$h = tan(\beta^m)$$
$$* \sqrt{tan^2(\alpha^m) * [d_y - (r - rcos\theta_m)]^2 + [d_y - (r - rcos\theta_m)]^2} \quad (12)$$

Then the channel vector of user k in UCA massive MIMO system using SW can be obtained as eq. (7). As for AAoA and EAoA, we also use the uniform distribution with certain azimuth angle spread (AAS) and elevation angle spread (EAS)

$$p(\Theta) = \frac{1}{2\Delta\Theta}, -\Delta\Theta + \Theta_0 \leq \Theta \leq \Delta\Theta + \Theta_0 \quad (13)$$

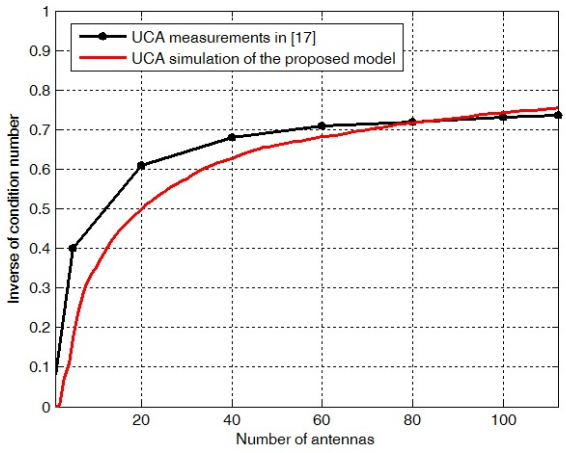

Fig. 3. UCA massive MIMO system condition number compared with measurements.

where $\Delta\Theta$ is the AAS/EAS, and Θ_0 is the mean AAoA/EAoA.

Fig. 3 compares the UCA massive MIMO system condition number (condition number is defined as the ratio between the largest eigenvalue value σ_{max} and the smallest eigenvalue value σ_{min} of $\mathbf{H}^H\mathbf{H}$ [17]) with the measurements in [17]. We set the channel parameters according to the measurements settings and environment in [17] strictly. The measurements were conducted in outdoor campus environment, where the BS antenna is 112 uniform cylindrical array with $\lambda/2$ antenna spacing on the top of a large building and $K = 2$. Both AAS and EAS are set to be 30° due to the residential urban area environment, and d_y is set to be 1000λ because the BS antennas are not far from the measurements positions. Fig. 3 shows that the simulation results are in good agreement with the measured data.

III. 3D Geometrical Channel Modeling for URA Massive MIMO System

The URA is another popular antenna structure in massive MIMO system. As shown in Fig. 4, both the horizontally and vertically antenna spacings are d [13]. The channel model analysis of URA massive MIMO system is a little more complex. In like manner, we first analyze the relationship between two antennas A_{11} and A_{mn} as shown in Fig. 5. The exact distances between the signal scattering point S and the

$$\mathbf{h}_k^{UCA} = \begin{bmatrix} h_{1,k}^{UCA} \\ ... \\ h_{m,k}^{UCA} \\ ... \\ h_{M,k}^{UCA} \end{bmatrix} = \begin{bmatrix} A_k e^{j(\phi_k+2\pi\sqrt{d_{x,k}^2+d_{y,k}^2+h_k^2}/\lambda)} \\ ... \\ A_k e^{j(\phi_k+2\pi\sqrt{(rsin\theta_m+d_{x,k})^2+[d_{y,k}-(r-rcos\theta_m)]^2+h_k^2}/\lambda)} \\ ... \\ A_k e^{j(\phi_k+2\pi\sqrt{(rsin\theta_M+d_{x,k})^2+[d_{y,k}-(r-rcos\theta_M)]^2+h_k^2}/\lambda)} \end{bmatrix} \quad (7)$$

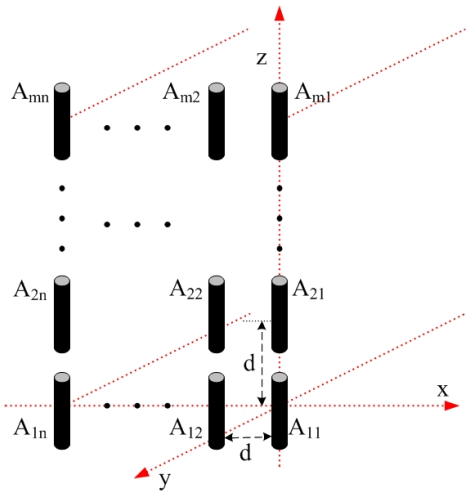

Fig. 4. Antenna array structure of URA massive MIMO system.

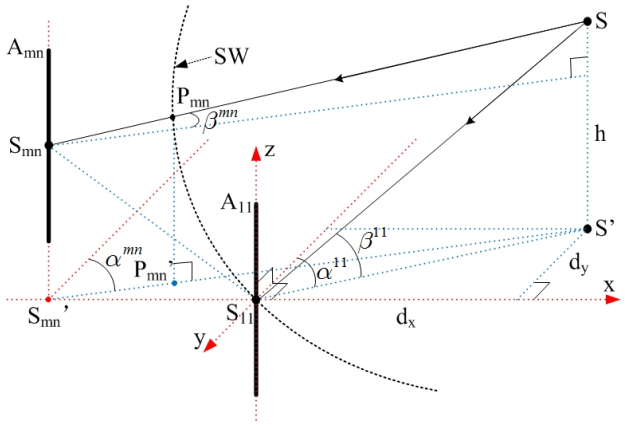

Fig. 5. 3D URA massive MIMO system communication scenario using SW.

two antennas are

$$SS_{11} = \sqrt{(d_x^2 + d_y^2 + h^2)}$$

$$SS_{mn} = \sqrt{(S_{11}S'_{mn} + d_x)^2 + d_y^2 + (h - S_{mn}S'_{mn})^2} \quad (15)$$

where $S_{mn}S'_{mn}$, $S'_{mn}S_{11}$ are the multiples of the antenna spacing. Regarding antenna A_{11} as a reference antenna, the channel of antenna A_{11} and A_{mn} can be expressed as

$$h_{mn}^{URA} = Ae^{j(\phi + 2\pi\sqrt{(d_x^2+d_y^2+h^2}/\lambda)} \quad (16)$$

$$h_{mn}^{URA} = Ae^{j(\phi + 2\pi\sqrt{((n-1)d+d_x)^2+d_y^2+(h-(m-1)d)^2}/\lambda)} \quad (17)$$

According to the geometrical relationship in Fig. 5, we can obtain

$$d_x = tan(\alpha^{mn}) * d_y - (n-1)d$$

$$h = tan(\beta^{mn})\sqrt{tan^2(\alpha^{mn})d_y^2 + d_y^2} + (m-1)d \quad (18)$$

Then we can get the channel vectors of user k in URA massive MIMO system as eq. (14). Fig. 6 compares channel capacity of URA massive MIMO system with the measurements in [18]. The transmitter is 256 URA on the top of a high building and the receiver is 16 antennas to form 256×16 massive MIMO system. [18] also showed the measured AAS/EAS, and we set the channel parameters according to the measured data. AAS is 20.89°, EAS is 10.47° and the antenna spacing is half-wavelength. Fig. 6 shows that the simulation results

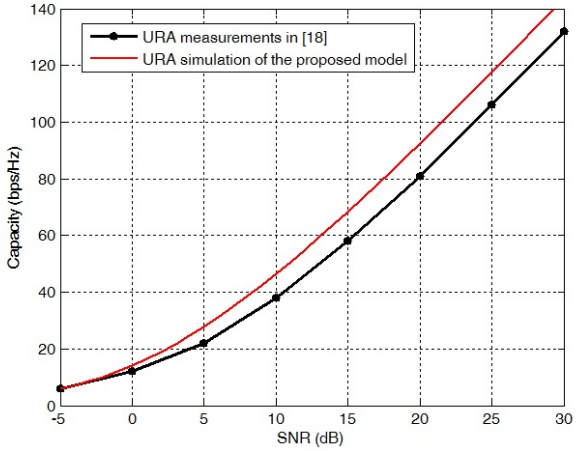

Fig. 6. Channel capacity of URA massive MIMO system vs SNR

can match the measured data, and there is small difference between simulation results and the measurements. This is because in the measurements campaign, all the antennas are multi-polarized antennas, while in our models we did not consider the multi-polarized antennas

IV. Simulation Results and Analysis

For the parameters of AAS and antenna spacing, the UCA and URA massive MIMO systems have the same performance as ULA massive MIMO system as shown in [12]. We focus on the comparison of three kinds of massive MIMO systems. Fig.

$$\mathbf{h}_k^{URA} = \begin{bmatrix} h_{11,k}^{URA} \\ h_{12,k}^{URA} \\ \cdots \\ h_{21,k}^{URA} \\ \cdots \\ h_{mn,k}^{URA} \end{bmatrix} = \begin{bmatrix} A_k e^{j(\phi_k + 2\pi\sqrt{d_{x,k}^2+d_{y,k}^2+h_k^2}/\lambda)} \\ A_k e^{j(\phi_k + 2\pi\sqrt{(d+d_{x,k})^2+d_{y,k}^2+h_k^2}/\lambda)} \\ \cdots \\ A_k e^{j(\phi_k + 2\pi\sqrt{d_{x,k}^2+d_{y,k}^2+(h_k-d)^2}/\lambda)} \\ \cdots \\ A_k e^{j(\phi_k + 2\pi\sqrt{((n-1)d+d_{x,k})^2+d_{y,k}^2+(h_k-(m-1)d)^2}/\lambda)} \end{bmatrix} \quad (14)$$

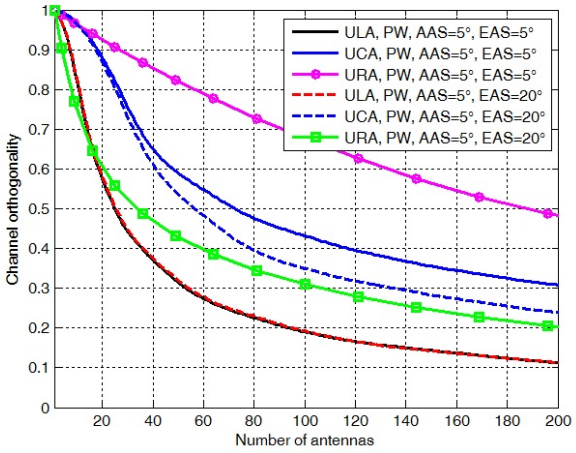

Fig. 7. Channel orthogonality of three massive MIMO systems vs number of antennas with different EAS.

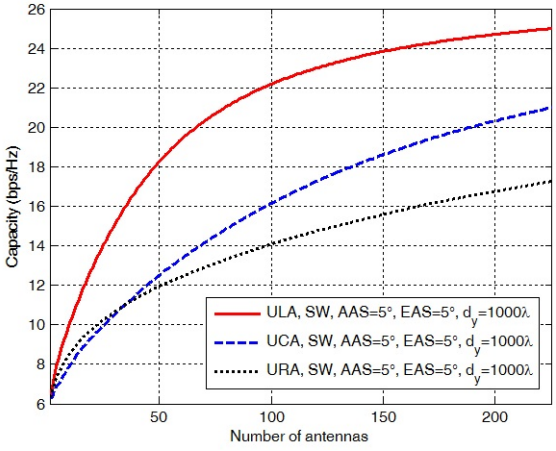

Fig. 9. Channel capacity of three massive MIMO systems vs number of antennas using SW.

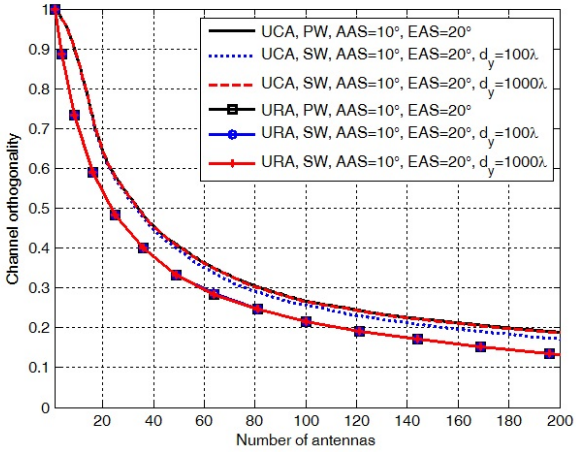

Fig. 8. Channel orthogonality of UCA and URA massive MIMO systems vs number of antennas using both PW and SW.

7 compares the channel orthogonality of three massive MIMO systems vs. number of antennas with different EAS. We use the square antennas structure by setting $m = n$ in URA massive MIMO system. From Fig. 7 we can see that the ULA massive MIMO system has the lowest channel orthogonality because of the huge antennas array, while the URA massive MIMO system has the highest channel orthogonality due to the compact antennas structure. Different from the ULA massive MIMO system, the channel orthogonality of UCA and URA massive MIMO systems is also sensitive to the EAS, and a larger EAS results in a lower channel orthogonality. This is because the UCA and URA massive MIMO systems are two dimensional antennas structure placed in the horizontal or vertical plane, which can develop the degree of freedom in the vertical direction. The channel orthogonality of URA massive MIMO system is more sensitive to the EAS than UCA massive MIMO system, and the channel orthogonality of URA massive MIMO system declines a lot as EAS gets larger compared with UCA massive MIMO system. Fig. 8 compares the channel orthogonality of UCA and URA massive MIMO systems vs. number of antennas using both PW and SW. For UCA massive MIMO system, the channel orthogonality performance has the same characteristics as the ULA massive MIMO system. The SW curves overlap the PW curve when the number of antennas is small. As the number of antennas increases, the channel orthogonality using the PW and SW becomes different. As the distance between the scattering point and the BS antennas becomes larger, the SW curve gets closer to the PW curve, which means the SW effect is weakened as the distance between the scattering point and the BS antennas becomes larger. For URA massive MIMO system, the SW curves always overlap the PW curve even when the number of antennas is large and the distance between the scattering point and the BS antennas is small, which means the SW effect is very weak for the URA massive MIMO system because the URA massive MIMO system has a compact antennas structure. Fig. 9 shows the channel capacity of three massive MIMO systems using SW. SNR is set to be 10 dB, $K = 8$ and the power is uniformly allocated. As the number of antennas increases, all the channel capacities increase to a certain extent and to continue adding antennas makes very little improvement such as beyond 100 antennas. With the lowest channel orthogonality, the ULA massive MIMO system has the highest channel capacity. While the URA massive MIMO system has the lowest channel capacity because of the highest channel orthogonality.

Finally, we compare and summarize the performance of antenna array structures for three massive MIMO systems as shown in TABLE I. The ULA massive MIMO system can make full use of space degree of freedom due to the large antenna array to achieve the best performance. However, the ULA is very difficult to be installed and placed on BS due to the large antenna array. For example, a 100-ULA antenna

TABLE I
PERFORMANCE COMPARISON OF ANTENNA ARRAY STRUCTURES OF THREE PROPOSED MASSIVE MIMO SYSTEMS.

Antennas array structure	Array size	Azimuth angle spread	Elevation angle spread	Antenna spacing	Spherical wave effect	Channel orthogonality	Capacity	Placement
ULA	Large	Sensitive	Insensitive	Sensitive	Strong	Low	High	Difficult
UCA	Medium	Sensitive	Medium	Sensitive	Medium	Medium	Medium	Easy
URA	Compact	Sensitive	Sensitive	Sensitive	Weak	High	Low	Easy

at 2.5 GHz with half-wavelength antenna spacing can reach 5.94 m, which is really hard to be put on the BS. The UCA massive MIMO system outperforms the URA massive MIMO system in many communication scenarios and is easy to be installed and placed. While the URA massive MIMO system is also sensitive to the EAS by developing the degree of freedom in the vertical direction, and the SW effect is very weak for URA antenna because of the compact antenna structure. For instance, a 10×10 URA antenna at 2.5 GHz with half-wavelength antenna spacing only needs 0.29 square meters, which is also easy to be placed and implemented relative to ULA antenna array. Therefore, it is important to choose the appropriate antenna array structures according to the communication scenarios and requirements, and TABLE I gives some guidelines.

V. CONCLUSION

In this paper, 3D geometrical channel models are established in UCA and URA massive MIMO systems. The proposed channel models comprise the parameters of communication environment and antennas such as scattering status, near-field effect, antennas array structures etc, which can be adjusted according to the communication environment and are easy to be implemented. We focus on the comparison of three types of massive MIMO systems. The ULA massive MIMO system has the best performance, and the UCA massive MIMO system outperforms the URA massive MIMO system in many communication scenarios. The URA massive MIMO system is also sensitive to the EAS by developing the degree of freedom in the vertical direction, and the SW effect is very weak for URA antennas array because of the compact antennas structure.

ACKNOWLEDGEMENT

This work is supported in part by the National Natural Science Foundation of China under Grant 61372077, and in part by the Shenzhen Science and Technology Program under Grants JCYJ 20170302150411789, JCYJ 20170302142515949, GCZX 2017040715180580, GJHZ 20180418190529516, JSGG20180507183215520.

REFERENCES

[1] H. A. Omar, K. Abboud, N. Cheng, K. R. Malekshan, A. T. Gamage and W. Zhuang, "A Survey on High Efficiency Wireless Local Area Networks: Next Generation WiFi," *IEEE Communications Surveys and Tutorials*, vol. 18, no. 4, pp. 2315-2344, Apr. 2016.

[2] Z. Ankarali, B. Pekoz and H. Arslan, "Flexible Radio Access Beyond 5G: A Future Projection on Waveform, Numerology, and Frame Design Principles," *IEEE Access*, vol. 5, pp. 18295-18309, Mar. 2017.

[3] S. Wu, C. Wang, el-Hadi M. Aggoune, M. M. Alwakeel and Y. He, "A Non-Stationary 3-D Wideband Twin-Cluster Model for 5G Massive MIMO Channels," *IEEE Journal on Selected Areas in Communications*, vol. 32, no. 6, pp. 1207-1218, June 2014.

[4] S. Wu, C. Wang, H. Haas, el-Hadi M. Aggoune, M. M. Alwakeel and B. Ai, "A Non-Stationary Wideband Channel Model for Massive MIMO Communication Systems," *IEEE Transactions on Wireless Communications*, vol. 14, no. 3, pp. 1434-1446, Oct. 2014.

[5] Y. Xie, B. Li, X. Zuo, M. Yang and Z. Yan, "A 3D geometry-based stochastic model for 5G massive MIMO channels," *in Proc. 2015 11th International Conference on Heterogeneous Networking for Quality, Reliability, Security and Robustness (QSHINE)*, Nov. 2015, pp. 216-222.

[6] S. Wu, C. Wang, E. M. Aggoune and M. M. Alwakeel, "A novel Kronecker-based stochastic model for massive MIMO channels," *in Proc. 2015 IEEE/CIC International Conference on Communications in China (ICCC)*, Apr. 2016, pp. 1-6.

[7] C. F. Lopez, C. Wang and R. Feng, "A novel 2D non-stationary wideband massive MIMO channel model," *in Proc. 2016 IEEE 21st International Workshop on Computer Aided Modelling and Design of Communication Links and Networks (CAMAD)*, Dec. 2016, pp. 207-212.

[8] C. F. Lpez and C. Wang, "Novel 3-D Non-Stationary Wideband Models for Massive MIMO Channels," *IEEE Transactions on Wireless Communications*, vol. 17, no. 5, pp. 2893-2905, Feb. 2018.

[9] L. Liu, D. W. Matolak, C. Tao, Y. Li, B. Ai and H. Chen, "Channel capacity investigation of a linear massive MIMO system using spherical wave model in LOS scenarios," *Science China Information Sciencess*, vol. 59, no. 2, pp. 1-15, Feb. 2016.

[10] Y. Chen, Y. Li, S. Sun, X. Cheng and X. Chen, "A twin-multi-ring channel model for Massive MIMO system," *in Proc. 2016 16th International Symposium on Communications and Information Technologies (ISCIT)*, Sept. 2016, pp. 606-610.

[11] K. Zheng, S. Ou and X. Yin, "Massive MIMO channel models: A survey," *International Journal of Antennas and Propagation*, vol. 11, pp. 1-10, 2014.

[12] X. Cheng and Y. He, "Channel Modeling and Analysis of ULA Massive MIMO Systems," *in Proc. 2018 20th International Conference on Advanced Communication Technology (ICACT)*, Feb. 2018, pp. 411-416.

[13] T. Yang, R. Zhang, X. Cheng and L. Yang, "Secure Massive MIMO Under Imperfect CSI: Performance Analysis and Channel Prediction," *IEEE Transactions on Information Forensics and Security*, vol. 14, no. 6, pp. 1610-1623, Nov. 2018.

[14] J. Flordelis, F. Rusek, X. Gao, G. Dahman, O. Edfors and F. Tufvesson, "Spatial Separation of Closely-Located Users in Measured Massive MIMO Channels," *IEEE Access*, vol. 16, pp. 40253-40266, July 2018.

[15] X. Gao, O. Edfors, F. Rusek and F. Tufvesson, "Massive MIMO Performance Evaluation Based on Measured Propagation Data," *IEEE Transactions on Wireless Communications*, vol. 14, no. 7, pp. 3899-3911, Mar. 2015.

[16] S. Kwon and G. L. Stüber, "Geometrical Theory of Channel Depolarization," *IEEE Transactions on Vehicular Technology*, vol. 60, no. 8, pp. 3542-3556, Oct. 2011.

[17] J. Hoydis, C. Hoek, T. Wild and S. Brink, "Channel measurements for large antenna arrays," *in Proc. 2012 International Symposium on Wireless Communication Systems (ISWCS)*, Oct. 2012, pp. 811-815.

[18] Z. Zheng, J. Zhang, Y. Yu, L. Tian and Y. Wu, "Propagation characteristics of massive MIMO measurements in a UMa scenario at 3.5 & 6 GHz with 100 & 200 MHz bandwidth," *in Proc. 2017 IEEE 28th Annual International Symposium on Personal, Indoor, and Mobile Radio Communications (PIMRC)*, Feb. 2018, pp. 1-5.